Electronic Motion and Path Study in Presence of Varying Electric Field Using SciLab 6.1.1 for Coupled Differential Equations

Ravindra Singh*, Shiv Shankar Gaur

Department of Physics, Shivaji College (University of Delhi), Raja Garden New Delhi-110027.

Volume 1, Issue 2, March 2024
Received:9 January, 2024; Accepted: 4 March, 2024
DOI: https://doi.org/10.63015/5c-2412.1.2

Corresponding author email: ravindrasingh@shivaji.du.ac.in

Abstract: The study of electronic motion of the electron and its path has been investigated using coupled linear differential equations in presence of electric field. The program executed using Scilab for the electronic motion. 2-D & 3-D trajectories of the electronic path and the variation and the distances in x & y directions with constant Electric field studied. Plotting of trajectories successfully done with Scilab software 6.1.1. Here L.T and with D'operator methods shows same results. 3-D trajectory of the electronic motion is periodic at particular frequencies; along y direction the electrons gain more energy and having more potential with increasing frequency and the investigation of oscillations under given conditions is found to be much higher.

Keywords: Scilab software 6.1.1 and electronic motion.

1. Introduction: The new approaches of the electron path had been studied in the last three decades very fast. Everywhere in this universe there is existence of the electronic motion. The electronic path motion is different in liquid nano plasma and liquid magnetite plasma. The electrons are negatively-charged particles having mass that is approximately 1/1836 that of the proton and behave dual nature. The electronic world is everywhere in the form of mobile phones, software, electronic music, radio and television broadcasting, the electrical energy grid, air and space travel, engineering communications and a wide range of other areas. The study of electrons path with an experiment done and which interferes in the same manner as water, acoustical or light waves do [1-2]. The e/m, the ratio for e/m is 1.758820×10^{11} C/kg. Two simulation modules also can be used to find the value of e/m ratio for an electron. The electronic path is capable to send the signals from one part of machine to another. Electrical resistivity of metal wires shows that it increases as their width decreases [3-5]. The simulation of electron and particle in cell are very important these days. The mean free path λ of electron and carrier relaxation time τ of the twenty most conductive elemental metals are determined by numerical integration over the Fermi surface obtained from first-principles, using constant λ or τ approximations and wave-vector dependent Fermi velocities $v_f(\boldsymbol{k})$ [6]. The path of a particle of mass m carrying a charge e is determined by the author (Herbert Stanley Allen) in combined magnetic and electric fields, when the lines of force are radial and are such as might be due to a single pole of strength μ coincident with an electric charge k [7]. The electrons orbiting around their common barycenter can form bound states and have a triplet spin structure which is independent of the center-of-mass momentum [8]. The resonance in spin can be induced by high-frequency electric fields in materials with a spin–orbit interaction; the oscillation of the electrons creates a momentum-dependent effective magnetic field acting on the electron spin [9-12]. The electron cyclotron drift instability driven by the electron $E \times B$ drift in partially magnetized plasmas that is investigated by Salomon Janhunen et.al. instability is so highly, resolved particle-in-cell simulations [13]. The existence of intense nonstationary processes in helical electron beams (HEB) is done experimentally by [14-15] and the study of helical electron beams (HEB) with disturbed axial symmetry of currents density and HEB with locking electrons in magnetic trap done by A. N. Kuftin et.al.

2. General Discussion: The path of an electron in a magnetic field is shown in figure 1 for which the magnetic force can be find by using the formula $Bev = mv^2/r$ where B is the magnetic field of strength, e is the electronic charge and v is the

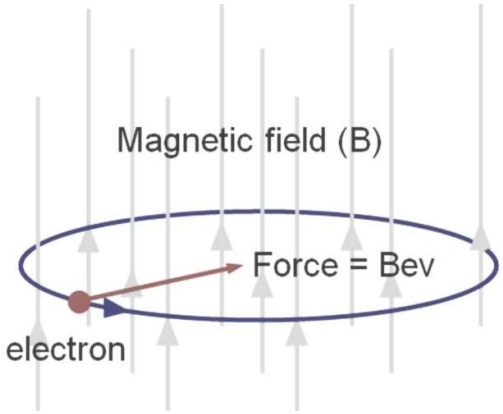

Figure 1: The path of an electron in presence of magnetic field

electron velocity. In a magnetic field the force is always at right angles to the motion of the electron (Fleming's left-hand rule) and so it shows that the path of the electron is circular as shown in Figure 2. Suppose the electron enters the field at an angle to the field direction then the path of the electron will be helical as shown in figure 3.

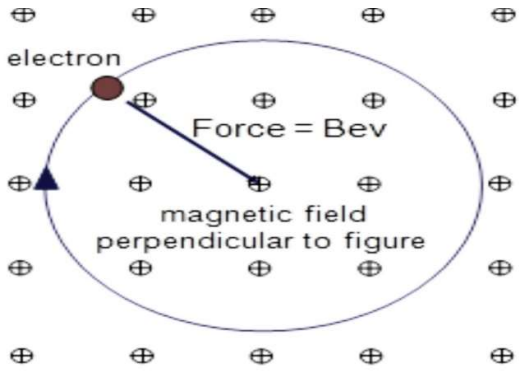

Figure 2: Circular path of the electron

The path of the electron in an electric field is given by the equation, $y = [\, Ev/2mdv^2 \,] x^2$ where V is the potential difference between the plates which are are aligned along the x direction and the electron enters the field at right angles to the field lines and x = vt then the force equation on the electron is given by the equation: F = eE = eV/d = ma. Mass and charge of the electron respectively; mass of the electron, m = 9.1 x 10^{-31} kg and the charge of the electron, e = 1.6 x 10^{-19} J. So above is the is the equation of a parabola since for a given electron velocity y is proportional to x^2. Figure 1 reveals about the motion of a charged particle in a uniform magnetic field having magnitude F=qvBsinθ is acted where θ is the angle of velocity **v** with the magnetic field **B**. It was the general discussion about the electron path. Now we focused on the equation of motion for the path of electron obtained by the coupled differential solved analytically. Now ignoring the magnetic effect.

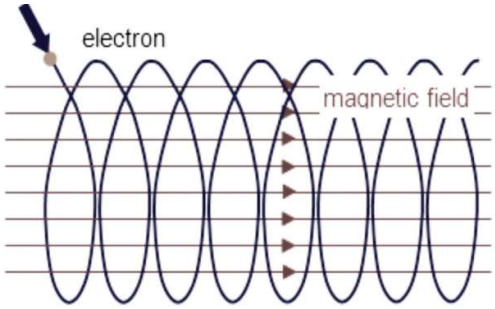

Figure 3: Helical motion of the electron

Here we are taking into account only Electric-field.

3. Electron Dynamics: Here we have to study of the path of electron for a set of coupled differential equations given below

$$m\frac{d^2x}{dt^2} + eh\frac{dy}{dt} = eE \qquad \text{……..(1)}$$

$$m\frac{d^2y}{dt^2} + eh\frac{dx}{dt} = B \qquad \text{……..(2)}$$

with conditions $x = \frac{dx}{dt} = y = \frac{dy}{dt} = 0$. Where m is the mass of the electron, m = 9.1 x 10^{-31} kg and the electronic charge, e = 1.6 x 10^{-19} C; x & y are the position coordinates.

Solution of the Equations: Solving equations (1) and (2); multiplying (2) by ξ (when magnetic field is zero) and adding to (1), we get

$$m\frac{d^2x}{dt^2} + m\xi\frac{d^2y}{dt^2} + eh\frac{dy}{dt} - eh\xi\frac{dx}{dt} = eE$$

$$m\frac{d^2}{dt^2}(x + \xi y) - eh\xi\frac{d}{dt}\left(-\frac{y}{\xi} + x\right) = eE \text{…..(3)}$$

Let us choose a parameter such that $x + \xi y = x - \frac{y}{\xi}$ on solving we get $\xi = \pm i$. Once we put $x + \xi y = \psi$ in (3), we have

$$m\frac{d^2\psi}{dt^2} - eh\xi\frac{d\psi}{dt} = eE$$

$$\frac{d^2\psi}{dt^2} - \omega\xi\frac{d\psi}{dt} = \frac{eE}{m} \qquad \text{…..(4)}$$

The complete solution is given by

$\psi = c_1 + c_2\, e^{\omega\xi t} - \frac{Et}{h\xi}$ as $x + \xi y = \psi$ then we can write

$$x + \xi y = c_1 + c_2\, e^{\omega\xi} - \frac{Et}{h\xi} \quad \text{.....(5)}$$

In equation (5) putting the value of $\xi\ i.e. i = -i$, *we get*

$$x + iy = c_1 + c_2\, e^{i\omega t} - \frac{Et}{ih} \quad \text{.....(6)}$$

$$x - iy = c_3 + c_4\, e^{-i\omega t} + \frac{Et}{ih} \quad \text{.....(7)}$$

The differentiation of above equations (6) and (7) takes form

$$\frac{dx}{dt} + i\frac{dy}{dt} = c_2\, i\omega e^{i\omega t} + \frac{iE}{h} \quad \text{.....(8)}$$

$$\frac{dx}{dt} - i\frac{dy}{dt} = -\, i\omega c_4 e^{-i\omega t} - \frac{iE}{h} \quad \text{.....(9)}$$

Now using initial conditions, $x = y = \frac{dx}{dt} = \frac{dy}{dt} = 0$ when t = 0 in (6), (7), (8) and (9), we get

$$\boldsymbol{x = \frac{E}{h\omega}\,[1 - \cos(\omega t)]} \quad \text{.....(12)}$$

$$\boldsymbol{y = \frac{E}{h\omega}\,[\omega t - \sin(\omega t)]} \quad \text{.....(13)}$$

Equations (12) and (13) represents the equations of the path for electron for given set of coupled differential equations. Further we solve the equations using Laplace transform. Let the Laplace transform of x be $\mathcal{L}[x] = \bar{x}$ and $\mathcal{L}[y] = \bar{y}$.

$\mathcal{L}\left[\frac{d^2x}{dt^2}\right] = p^2\,\mathcal{L}[x] - p\,x(0) - \dot{x}(0)$ and

$\mathcal{L}\left[\frac{d^2y}{dt^2}\right] = p^2\,\mathcal{L}[y] - p\,y(0) - \dot{y}(0)$

$\mathcal{L}\left[\frac{dx}{dt}\right] = p\bar{x} - x(0)$ and $\mathcal{L}\left[\frac{dy}{dt}\right] = sp - y(0)$

$$p^2\bar{x} - px(0) - \dot{x}(0) + \frac{eh}{m}[p\bar{y} - y(0)] = \frac{eE}{mp} \quad \text{---- (14)}$$

$$p^2\bar{y} - p\,y(0) - y'(0) - \frac{eh}{m}[p\bar{x} - x(0)] = 0 \quad \text{--- (15)}$$

Now use the given conditions $x(0) = 0$; $\dot{x}(0) = 0$ & $y(0) = 0$; $\dot{y}(0) = 0$ above equations takes form

Figure 4: Shows the variation of path 'E' Vs 'r2' (a) ω=π/2; (b) ω=π/3

$$p^2\bar{x} + \frac{eh}{m}[p\bar{y}] = \frac{eE}{mp} \quad \text{----- (16)}$$

and $p^2\bar{y} - \frac{ehp\bar{x}}{m} = 0$ ----- (17)

Solving above equations for x and y we get

$\bar{x} = -\left(\frac{eE}{m}\right)\frac{1}{p\left(p^2 + \left(\frac{eh}{m}\right)^2\right)}$ and

$\bar{y} = -\,(Eh)\left(\frac{e}{m}\right)^2\frac{1}{p^2\left(p^2 + \left(\frac{eh}{m}\right)^2\right)}$

Now the result given below has been solved by using partial fractions.

$$x = -\left(\frac{eE}{m}\right)\{L^{-1}[-\left(\frac{m}{eh}\right)^2.\frac{1}{p}] + L^{-1}[\left(\frac{m}{eh}\right)^2.\frac{p}{p^2 + \left(\frac{eh}{m}\right)^2}]\} \quad \text{------ (18)}$$

$$y = \frac{E}{h}\left[t - \frac{m}{eh}\sin\left(\frac{eh}{m}\right)t\right] \quad \text{----- (19)}$$

Put $\omega = \frac{eh}{m}$ in above equations we have

$$\boldsymbol{x = \frac{E}{h\omega}[1 - \cos(\omega t)]} \quad \text{---- (20)}$$

$$\boldsymbol{y = \frac{E}{h\omega}[\omega t - \sin(\omega t)]} \quad \text{----- (21)}$$

Equations (20) and (21) represents the equations of the path for electron for given set of coupled differential equations. On comparing four equations (12) & (20); (13) and (21) are found to be same. Next we analyzed the same equations

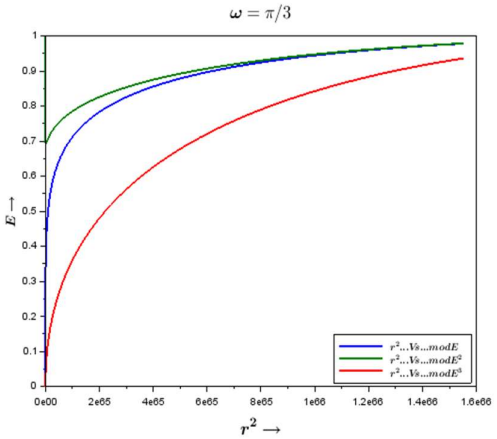

using Scilab software.

4. Results: Figure 4 is the variation of Electric

field, E and r^2 where $r = \sqrt{x^2 + y^2}$. Here it is observed that E increases with respect to r at some frequencies ω=π/2 & ω=π/3. Electric field is proportional to distance. When r is very high then a saturation is found for all the curves for limited time. The sharp result comes out when ω=π/2 for large 't' the plot line converts into a tedious path like scattering of particles. Green line is the curve between 'r^2' Vs 'modulus of E'.

Figure 5(a)-5(d) represents electron trajectory in the *x* – *y* plane. The plots of both solutions are against one another at a constant value of field, increasing in equal steps and the frequency is also increasing from 5(a)-5(d). The plots show the variation of x and y for a fixed value of time for

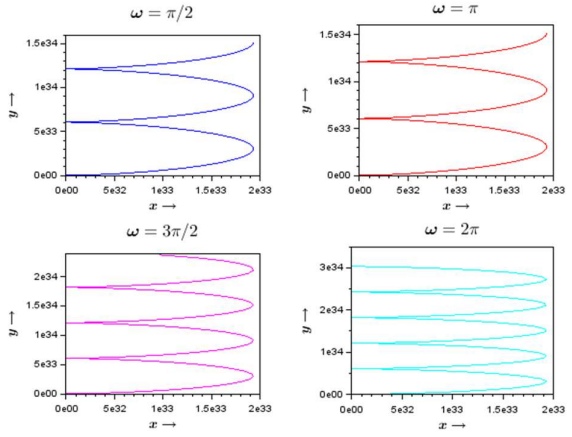

Figure 5: Shows the variation of path y Vs x. For (a) ω=π/2; (b) ω=π; (c) ω=3π/2; and (d) ω=2π.]

each. Mathematically it is noticed from the graph that y is multivalued function, angular frequency doesn't matter in this case here. So it is observed that along y direction the electrons gains more energy or having more potential with increasing frequency and the oscillations under some conditions are found to be much higher. The Hamiltonian as well as the momentum and kinetic energy attains high value in y direction. The classical theoretical aspects are also valid here. If we use variational process, we can restrict the comparison of all paths involving no violation of conservation of energy and momentum also the Hamiltonian, H will be conserved.

Figure 6(a)-6(c) represents 3D electron trajectory. The 3-D trajectory has been studied with the help of latest Scilab software for particular values of angular frequencies ω=π/2, ω=π/3 and ω=π/4. 3-D trajectory depends upon the angular frequency; in the study it has been found that on decreases the angular frequency there is increment in trajectory loops and the separation between them becomes so close and looks like spiral or human ribs shape.

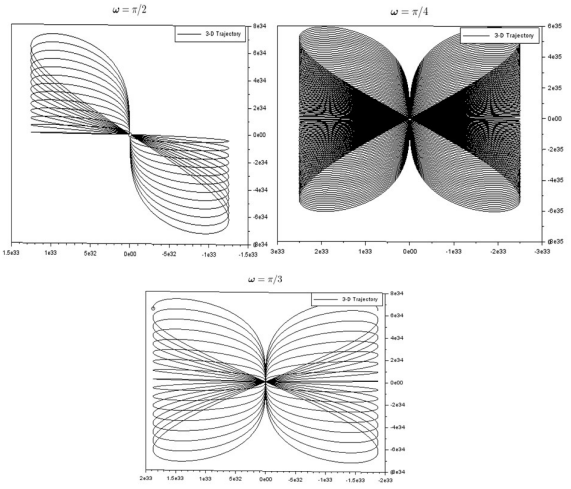

Figure 6: Shows the variation of path y Vs x. For (a) ω=π/2; (b) ω=π; (c) ω=3π/2.

The figure formed from the trajectory is found to be symmetry with respect to x and y and also about y=x at some particular angular frequencies.

Scilab Coding: Scilab programming/coding done successfully. The coding of Scilab for figure 4 follows as:

```
clc;
funcprot(0);
e=(1.6)*1e-19;
h=(6.6)*1e-34;
m=(9.1)*1e-31;
w=%pi/2;
t=linspace(0,1.3,500);
E=sin(ws.*t);
x=(E/(h.*w)).*(1-cos(w.*t));
y=(E/(h.*w)).*(w.*t-sin(w.*t));
r=sqrt(x.^2+y.^2);
plot(r.^2,abs(E),r.^2,abs(E.^E),r.^2,abs(E.^3),'thickness',
2)
xstring(5e34,-.5,["(a)"],0,1)
xlabel('$\boldsymbol{r^2\rightarrow}\$','fontsize',4)
ylabel('$\boldsymbol{E\rightarrow}\$','fontsize',3)
legend('$\boldsymbol{r^2...Vs...mod
E\$','$\boldsymbol{r^2...Vs...mod
E^2\$','$\boldsymbol{r^2...Vs...mod E^3\$',4)

title('$\boldsymbol\text\omega=\pi/2$','fontsize',4)

clc;
funcprot(0);
e=(1.6)*1e-19;
h=(6.6)*1e-34;
m=(9.1)*1e-31;
w=%pi/3;
t=linspace(0,1.3,500);
E=sin(w.*t);
x=(E/(h.*w)).*(1-cos(w.*t));
```

```
y=(E/(h.*w)).*(w.*t-sin(w.*t));
r=sqrt(x.^2+y.^2);
plot(r.^2,abs(E),r.^2,abs(E.^E),r.^2,abs(E.^3),'thickness',
2)
xstring(5e34,-.5,["(a)"],0,1)
xlabel('$\boldsymbol{r^2\rightarrow}\$','fontsize',4)
ylabel('$\boldsymbol{E\rightarrow}\$','fontsize',3)
legend('$\boldsymbol{r^2...Vs...mod
E\$','$\boldsymbol{r^2...Vs...mod
E^2\$','$\boldsymbol{r^2...Vs...mod E^3\$',4)
title('$\boldsymbol\text\omega=\pi/3$','fontsize',4)
```

Scilab programming/coding done successfully. The coding of Scilab for figure 5 follows as

```
clc;
funcprot(0);
e=(1.6)*1e-19;
h=(6.6)*1e-34;
m=(9.1)*1e-31;
w=%pi/2;
E=1;
t=linspace(0,10,100);
x=(E/(h.*w)).*(1-cos(w.*t));
y=(E/(h.*w)).*(w.*t-sin(w.*t));
subplot(2,2,1)
plot(x,y,'thickness',1)
xstring(1e33,5.9e34,["(a)"],0,1)
xlabel('$\boldsymbol{x\rightarrow}\$','fontsize',3)
ylabel('$\boldsymbol{y\rightarrow}\$','fontsize',3)
title('$\boldsymbol\text\omega=\pi/2$','fontsize',4)
w=%pi;
E=2;
t=linspace(0,5,100);
x=(E/(h.*w)).*(1-cos(w.*t));
y=(E/(h.*w)).*(w.*t-sin(w.*t));
subplot(2,2,2)
plot(x,y,'r','thickness',1)
xstring(1e33,1.2e35,["(b)"],0,1)
xlabel('$\boldsymbol{x\rightarrow}\$','fontsize',3)
ylabel('$\boldsymbol{y\rightarrow}\$','fontsize',3)
title('$\boldsymbol\text\omega=\pi$','fontsize',4)
w=3*%pi/2;
E=3;
t=linspace(0,5,100);
x=(E/(h.*w)).*(1-cos(w.*t));
y=(E/(h.*w)).*(w.*t-sin(w.*t));
subplot(2,2,3)
plot(x,y,'m','thickness',1)
xstring(1e33,1.7e35,["(c)"],0,1)
xlabel('$\boldsymbol{x\rightarrow}\$','fontsize',3)
ylabel('$\boldsymbol{y\rightarrow}\$','fontsize',3)
title('$\boldsymbol\text\omega=3\pi/2 $','fontsize',4)
w=2*%pi;
E=4;
t=linspace(0,5,100);
x=(E/(h.*w)).*(1-cos(w.*t));
y=(E/(h.*w)).*(w.*t-sin(w.*t));
subplot(2,2,4)
plot(x,y,'c','thickness',1)
xstring(1e33,2.5e35,["(d)"],0,1)
xlabel('$\boldsymbol{x\rightarrow}\$','fontsize',3)
ylabel('$\boldsymbol{y\rightarrow}\$','fontsize',3)
title('$\boldsymbol\text\omega=2\pi$','fontsize',4)
```

Scilab programming/coding done successfully. The coding of Scilab for figure 6 follows as

```
clc;
funcprot(0);
e=(1.6)*1e-19;
h=(6.6)*1e-34;
m=(9.1)*1e-31;
w=%pi/2;
t=linspace(0,50,5000);
E=sin(w.*t);
x=(E/(h.*w)).*(1-cos(w.*t));
y=(E/(h.*w)).*(w.*t-sin(w.*t));
r=sqrt(x.^2+y.^2);
comet3d(t,x,y)
xstring(5e34,-.5,["(a)"],0,1)
legend('3-D Trajectory')
title('$\boldsymbol\text\omega=\pi/2$','fontsize',4)
```

```
clc;
funcprot(0);
e=(1.6)*1e-19;
h=(6.6)*1e-34;
m=(9.1)*1e-31;
w=%pi/3;
t=linspace(-50,50,10000);
E=sin(w.*t);
x=(E/(h.*w)).*(1-cos(w.*t));
y=(E/(h.*w)).*(w.*t-sin(w.*t));
r=sqrt(x.^2+y.^2);
comet3d(t,x,y)
xstring(5e34,-.5,["(a)"],0,1)
legend('3-D Trajectory')
title('$\boldsymbol\text\omega=\pi/3$','fontsize',4)
```

```
clc;
funcprot(0);
e=(1.6)*1e-19;
h=(6.6)*1e-34;
m=(9.1)*1e-31;
w=%pi/4;
t=linspace(-400,400,10000);
E=sin(w.*t);
x=(E/(h.*w)).*(1-cos(w.*t));
y=(E/(h.*w)).*(w.*t-sin(w.*t));
r=sqrt(x.^2+y.^2);
comet3d(t,x,y)
xstring(5e34,-.5,["(a)"],0,1)
legend('3-D Trajectory')
title('$\boldsymbol\text\omega=\pi/4$','fontsize',4)
```

5. Conclusions: The motion of the electron is determined for a set of coupled linear differential equation of second order under certain conditions with an electric field. The opted methods give the same result and verified with the software. The presence if the electric field is considered constant as well as in trigonometric form; the path of the electron is analyzed and the trajectories of the electron and the variation of r with E have been studied. Scilab software 6.1.1 used throughout the plotting and the problem is analysed with it. The

importance of the software is that it gives more accurate study of trajectories, variation with distance and symmetry with angular frequencies. Using Scilab the amplitude/oscillations under given conditions are found to be much higher for path, y. The momentum and kinetic energy found to be high in y direction as compared to x direction. 3-D trajectory depends upon the angular frequency and found to be symmetry with respect to x and y and also about y=x.

References:

1. Matija Karalic, Antonio Štrkalj, Michele Masseroni, Wei Chen, Christopher Mittag, Thomas Tschirky, Werner Wegscheider, Thomas Ihn, Klaus Ensslin, Oded Zilberberg, **"**Electron-Hole Interference in an Inverted-Band Semiconductor Bilayer", Physical Review **X**, 2020; 10 (3)
2. Journal of the Institution of Electrical Engineers IET **2** (14), 112 – 114 (1956).
3. R. L. Graham, G. B. Alers, T. Mountsier, N. Shamma, S. Dhuey, S. Cabrini, R. H. Geiss, D. T. Read, and S. Peddeti, "Resistivity dominated by surface scattering in sub-50nm Cu wires", Appl. Phys. Lett. **96**, 042116 (2010).
4. K. Barmak, A. Darbal, K. J. Ganesh, P. J. Ferreira, J. M. Rickman, T. Sun, B. Yao, A. P. Warren, and K. R. Coffey, "Surface and grain boundary scattering in nanometric Cu thin films: A quantitative analysis including twin boundaries", J. Vac. Sci. Technol. A **32**, 061503 (2014).
5. J. S. Chawla, F. Gstrein, K. P. O'Brien, J. S. Clarke, and D. Gall, "Electron scattering at surfaces and grain boundaries in Cu thin films and wires", Phys. Rev. B **84**, 235423 (2011).
6. Daniel Gall, "Electron mean free path in elemental metals", Journal of Applied Physics **119**, 085101 (2016); https://doi.org/10.1063/1.4942216
7. Herbert Stanley Allen, "The path of an electron in combined radial magnetic and electric fields", Memoirs of Fellows of the Royal Society **1**, 5–10 (1911).
8. Yasha Gindikin and Vladimir A. Sablikov, "Spin-orbit-driven electron pairing in two dimensions", Phys. Rev. B **98**, 115137 (2018).
9. Zavoisky, Y. K., "Spin magnetic resonance in para-magnetics", J. Phys. USSR **9**, 245–246 (1945).
10. Dyakonov, M. I. & Perel, V. I., "Spin relaxation of conduction electrons in non-centrosymmetric semiconductors", Sov. Phys. Solid State **13**, 3023–3026 (1972).
11. Rashba, E. I. & Efros, A. L., "Orbital mechanisms of electron-spin manipulation by an electric field", Phys. Rev. Lett. **91**, 126405 (2003).
12. Duckheim, M. & Loss, D., "Electric-dipole-induced spin resonance in disordered semiconductors", Nature Phys. **2**, 195–199 (2006).
13. S. Janhunen et.al., "Evolution of the electron cyclotron drift instability in two-dimensions", Physics of Plasmas **25**, 082308 (2018).
14. B.V. Raisky & S.E. Tsimring, "Numerical simulation of nonstationary processes in intense helical electron beams of gyrotrons", IEEE Transactions on Plasma Science **24**, 3 1996.
15. V. K. Lygin, V. N. Manuilov, B. V. Raisky, E. A. Solujanova & Sh. E. Tsimring , "Theory of helical electron beams in gyrotrons", International Journal of Infrared and Milli meter Waves **14**, 783–816 (1993).